Molecular Landscape of Anti-Drug Antibodies Reveals the Mechanism of the Immune Response Following Treatment with TNFα Antagonists

Running title: Molecular landscape of anti-drug antibodies

[1,†]Anna Vaisman-Mentesh, [1,†]Shai Rosenstein, [2]Miri Yavzori, [1]Yael Dror, [2]Ella Fudim, [2]Bella Ungar, [2]Uri Kopylov, [2]Orit Picard, [1]Aya Kigel, [2]Shomron Ben-Horin, [1]Itai Benhar, [1,*]Yariv Wine

[1] George S. Wise Faculty of Life Sciences, School of Molecular Cell Biology and Biotechnology, Tel Aviv University, Ramat Aviv, Israel

[2] Gastroenterology Department, Sheba Medical Center and Sackler School of Medicine, Tel-Aviv University, Tel Hashomer, Israel

[†] These authors have contributed equally to this work.

*Author for correspondence: Yariv Wine

yarivwine@tauex.tau.ac.il

Keywords: Immunogenicity, anti-drug antibodies, next generation sequencing, Ig-Seq, BCR-Seq, immune repertoire, antibody repertoire, proteomics, high-throughput sequencing, monoclonal antibody, biologics, therapeutic antibodies

Abstract

Drugs formulated from monoclonal antibodies (mAbs) are clinically effective in various diseases. Repeated administration of mAbs, however, elicits an immune response in the form of anti-drug-antibodies (ADA), thereby reducing the drug's efficacy. Notwithstanding their importance, the molecular landscape of ADA and the mechanisms involved in their formation are not fully understood. Using a newly developed quantitative bio-immunoassay, we found that ADA concentrations specific to TNFα antagonists can exceed extreme concentrations of 1 mg/ml with a wide range of neutralization capacity. Our data further suggest a preferential use of the λ light chain in a subset of neutralizing ADA. Moreover, we show that administration of TNFα antagonists result in a vaccine-like response whereby ADA formation is governed by the extrafollicular T cell-independent immune response. Our bio-immunoassay coupled with insights on the nature of the immune response can be leveraged to improve mAb immunogenicity assessment and facilitate improvement in therapeutic intervention strategies.

MAIN TEXT

Introduction

More than 30 years since the approval of the first therapeutic monoclonal antibody (mAb) for clinical use, the therapeutic mAb market has expanded exponentially, establishing mAbs as one of the leading biopharmaceutical therapeutic modalities (1). Although mAbs hold significant promise for improving human health, their repeated administration is often highly immunogenic and can elicit an undesirable anti-drug antibody (ADA) response (2). The formation of an ADA response interferes with the effect of the drug or neutralizes it thereby altering the drug's pharmacokinetic (PK) and pharmacodynamic (PD) properties and reducing its efficacy (3), and eventually may lead to a severe adverse immune reaction in humans (4).

Immunogenicity of mAbs and the formation of an ADA response has been suggested to be dependent on the interplay between factors related to the drug itself (e.g., non-human sequence, glycosylation, impurities, aggregation), to the patient (e.g., disease type, genetic factors, concomitant immunomodulators), or to the drug's route and frequency of administration (5, 6). However, the molecular mechanisms that lead to the induction of ADA are not well understood and were initially thought to be related to the murine origin of the mAbs because they were recognized as "non-self" by the human immune system. This idea propelled the mAb discovery field to focus on engineering refined mAbs by reducing the nonhuman portions and developing chimeric, humanized, and fully human mAbs by using human libraries or humanized mice at the mAb discovery phase (7).

Unfortunately, this strategy did not abolish the immunogenicity potential of mAbs and the associated induction of ADA. The question of why and how ADA develop is further complicated by data indicating that some patients develop ADA, and some do not, and by the observation that the extent of immunogenicity may differ among patients receiving the same mAb (8). ADA that develop in patients treated with an mAb can be stratified into two main categories: 1) neutralizing ADA (*nt*ADA) that directly block and interfere with the drug's ability to bind its target, and 2) non-neutralizing ADA (i.e., binding ADA *b*ADA) that recognize other epitopes on the drug while still retaining the mAb binding activity (9). *nt*ADA are generally considered to be more important in the clinical setting than *b*ADA because they directly reduce a drug's efficacy. However, *b*ADA may indirectly reduce the therapeutic efficacy of an mAb by compromising bioavailability or

accelerating drug clearance from the circulation. In both cases, *nt*ADA and *b*ADA substantially alter the PK and PD of the mAb being administered (10).

Originator and biosimilar tumor necrosis factor alpha (TNFα) antagonistic mAbs are used extensively in clinical settings to treat inflammatory bowel disease (IBD; e.g., Crohn's disease and ulcerative colitis), rheumatoid arthritis, and other chronic inflammatory associated disorders such as psoriasis, psoriatic arthritis, and ankylosing spondylitis (11). TNFα antagonists help reduce inflammatory responses by targeting both membrane-bound and soluble TNFα. Neutralizing soluble TNFα prevents its binding to its receptor and impedes the secretion and upregulation of the signal cascade, thereby inhibiting its biological activity. The binding of TNFα antagonists to transmembrane TNFα on immune effector cells causes their destruction by inducing cell apoptosis or cell lysis through reverse signaling (12).

Currently, five TNFα antagonists have been approved by both the U.S. Food and Drug Administration and the European Medicines Agency: infliximab (IFX), adalimumab (ADL), etanercept, golimumab, and certolizumab pegol (2). Additionally, several biosimilars have already been approved or are in various stages of development (13). Both IFX and ADL belong to the group of TNFα antagonists and are routinely used in clinical settings to treat inflammatory diseases. IFX is a chimeric mAb (75% human and 25% murine), whereas ADL is fully human. The reported immunogenicity extent of these drugs is inconsistent. Whereas pharmaceutical companies report 10–15% and 2.6–26% immunogenicity for IFX and ADL, respectively (14), clinical data suggest higher immunogenicity rates for these drugs (15). Patients treated with IFX and ADL can be stratified based on the characteristics of their response to treatment or lack thereof. Primary non-responders are patients whose disease does not respond to the drug at all, and a certain subset of these may be mediated via early formation of ADA (15, 16). Secondary non-responders are patients who initially respond to the drug but later fail treatment, often due to development of ADA (for IFX, this was reported to develop mostly within 12 months of treatment initiation) (16).

Studies reporting immunogenicity following mAb administration and ADA prevalence have been inconsistent due in part to the various assay formats used to monitor immunogenicity in the clinic (17). Current limitations of each available format might reduce utility in clinical and research settings and complicate data interpretation. Some assays have a poor dynamic range and may generate false negative results because of interfering interaction with another circulating drug, or conversely, false positive results due to the presence of other antibodies such as rheumatoid factor

(18). The pros and cons of available ADA detection assays were previously elaborated, and the formation of ADA following treatment with IFX, ADL, and other TNFα antagonists, including newly developed biosimilars, have been extensively studied and reviewed elsewhere (5, 19-21). Notwithstanding the effort invested in understanding the reasons that mAb immunogenicity and strategies to increase mAb efficacy, little is known about the molecular mechanism that governs the formation of ADA following treatment with an mAb.

In this study, we investigated the molecular landscape of ADA following treatment with TNFα antagonists. First, we developed a simple bio-immunoassay that accurately quantifies ADA levels in patient sera. We further modified the bio-immunoassay to evaluate the neutralization capacity of the ADA. Next, we aimed to profile the immune response following mAb administration. We used flow cytometry to determine the frequency of B cells in the circulation and whether the dynamics of the immune response was akin to vaccine response. Finally, we used next-generation sequencing (NGS) and high-resolution shotgun tandem mass spectrometry (LC-MS/MS) to elucidate the molecular composition of serum ADA. Using our bio-immunoassay we found that ADA levels in sera from 55 patients ranged between 2.7 and 1,268.5 μg/ml. The modified bio-immunoassay enabled us to differentiate between patients who have high and low neutralization capacity. Interestingly, we found that patients with a high neutralization capacity showed a strong bias in the λ/κ light chain ratio thereby suggesting that *nt*ADA exhibits a preference for λ light chains.

To elucidate the nature of the immune response following drug administration we chose to study a patient with IBD who was treated with IFX and who had high ADA levels and neutralization capacity. At 10 days (D10) following IFX infusion, the patient exhibited an approximately 13-fold increase in the frequency of plasmablasts (PB) and unchanged frequency of activated memory B cells (mBC), compared with the pre-infusion time point (D0). Comparative NGS analysis of the antibody heavy chain variable region (V_H) from isolated PB at D0 and D10, showed a significant temporal decrease in the level of somatic hypermutation (SHM) and an increase in the length of the complementary determining region 3 of the antibody heavy chain (CDRH3). Moreover, the proteomic analysis of serum ADA supports the observation obtained from the neutralization capacity assays, that a preference for using λ light chains exists. These data suggest a possible mechanism whereby the humoral immune response following the administration TNFα antagonists is governed by a T cell-independent (TI) response. This response may be induced by the formation of immunocomplexes (drug-TNFα-ADA) serving as a

strong driver of immunogenicity that in-turn diverts the immune response to TI pathway were B cells are activated by B cell receptor (BCR) cross-linking.

Materials and Methods

Over expression and purification of rhTNFα

The sequence-encoding residues Val77–Leu233 of human TNFα was cloned and fused to the N-terminal 6xHis tag in pET-28a+ vector (Novagen) and transformed into *Escherichia coli* Rosetta (DE3) cells (Novagen). A single colony was inoculated into 2ml LB supplemented with Kanamycin at final concentration of 100µg/ml and incubated over night (O.N.) at 37°C, 250 RPM. The culture was next re-inoculated into a 0.5L Erlenmeyer containing LB supplemented with Kanamycin, and grown at 37°C 250RPM until $O.D._{600}$~0.6-0.8 was reached. Induction was carried out by supplementing bacterial culture with IPTG (0.1mM final concentration) and incubating the culture for 3 hours at 37°C, 250RPM. Bacterial cells were harvested by centrifugation at 8000 RPM, 15 minutes, at 10°C (SORVALL RC6 Plus, Thermo Fisher Scientific) and cell pellet was stored O.N. at -20°C. Next, pellet was re-suspended in 30ml of binding buffer (50mM sodium phosphate buffer pH 8.0, 300mM NaCl, 10mM imidazole) and sonicated on ice for 8 cycles of 30 seconds pulse with 2-minute pause (W-385 sonicator, Heat Systems Ultrasonics). Following sonication, cells were centrifuged at 12000 RPM, 30 minutes, 4°C (SORVALL RC 6+) and supernatant was applied to a HisTrap affinity column (GE Healthcare) that was pre-equilibrated with binding buffer. All affinity purification steps were carried out by connecting the affinity column to a peristaltic pump with flow rate of 1/ml/min. Column was washed with 5 column volumes (CV) of wash buffer (50mM Sodium phosphate, pH 8.0, 300mM NaCl, 10% glycerol, 20mM imidazole) followed by elution of rhTNFα with 5CV of elution buffer (50mM Sodium phosphate, pH 6.0, 300mM NaCl, 10% glycerol, 500mM imidazole). Elution was collected in 1ml fractions and were analyzed by 12% SDS–PAGE. Fractions containing clean rhTNFα were merged and dialyzed using Amicon Ultra (Mercury) cutoff 3K against PBS (pH 7.4). Dialysis products were analyzed by 12% SDS–PAGE for purity and concentration was measured using Take-5 (BioTek Instruments). To test functionality of the produced rhTNFα, 96 well plate (Nunc MaxiSorp™ flat-bottom, Thermo Fisher Scientific) was coated with 1µg/ml (in PBS) of purified rhTNFα and commercial hTNFα (PHC3011, Thermo Fisher Scientific) and incubated at 4°C O.N. ELISA plates were then washed three times with PBST (0.1% v/v Tween 20 in PBS) and blocked with 300µl of 2% w/v BSA in PBS for 1 hour at 37^0C. Next, ELISA plates were washed three time with PBST, and incubated for 1 hour, room

temperature (RT) in triplicates with anti-TNFα mAb (Infliximab or Adalimumab) in 2% w/v BSA, PBS at the starting concentration of 50nM with 3-fold dilution series. Plates were then washed three times with PBST with 30 second incubation time at each washing cycle. For detection, 50µl of anti-human H+L HRP conjugated antibody (Jackson) was added to each well (1:5000 ratio in 2% w/v BSA in PBS) and incubated for 1 hour at RT, followed by three washing cycles with PBST. Developing was carried out by adding 50µl of 3,3',5,5'-Tetramethylbenzidine (TMB, Southern Biotech) and reaction was quenched by adding 50µl 0.1M sulfuric acid. Plates were read using the Epoch Microplate Spectrophotometer ELISA plate reader (BioTek Instruments).

Over expression and purification of IdeS

The coding sequence corresponding to amino acid residues 38–339 of *S. pyogenes* IdeS (numbered from the start of the signal sequence) was sub-cloned into the expression vector pET28b (Novagen). The coding sequencing was sub-cloned at the 3' end of Thioredoxin 6xHis-TEV. The complete construct was sub-cloned as previously described (45) and was kindly donated by Dr. Ulrich von Pawel-Rammingen from the Department of Molecular Biology, Umea University. The transformation of pET-TRX_b plasmid harboring the IdeS encoding gene (pET-IdeS) was carried out as follows: 200µl of chemical-competent *E. coli* BL21-DE3 cells were thawed on ice for 20 minutes. 50ng of the plasmid pET-IdeS was added to the thawed competent cells and incubated on ice for 20 minutes with gentle mixing every 5 minutes. Next, heat shock was applied by incubating the cells at 42°C for 2 minutes followed by incubation on ice water for 2 minutes. For phenotypic expression, 800µl of LB was added, and cells were incubated at 37°C, 250 RPM for 1 hour in a horizontal position. Cells were plated on LB agar supplemented with Kanamycin and incubated at 37°C overnight (O.N). Single colony was inoculated into 2ml LB supplemented with Kanamycin and incubated O.N. at 37°C, 250 RPM. Next day, 2ml from the grown cultures were inoculated into two 2liter flasks, each containing each 500ml LB supplemented with Kanamycin. Over expression and purification of IdeS was carried out as described for rhTNFα with a minor modification as follow: Ides was eluted with imidazole gradient (50, 150, 500mM imidazole), total of 20ml. 20 fractions of 1ml were collected from each elution step and evaluated for their purity using 12% SDS–PAGE. All fractions containing clean IdeS were merged and dialyzed O.N. at 4°C against 4L of PBS (pH 7.4), using SnakeSkin dialysis tubing with 10 kDa cutoff (Thermo Fisher Scientific). Dialysis products were analyzed by 12% SDS–PAGE.

Production of mAb-F(ab')$_2$

Intact clinical grade IFX or ADL (designated here as mAb) were digested using in-house produced IdeS. 10mg of mAb was incubated with 300µg of IdeS in the final volume of 500µl PBS for 2.5 hours at 37^{0}C, followed by a spike-in of additional 300µg of IdeS to achieve full digestion of the Fc fragments. IdeS inactivation was carried out by adding 0.1M of citric acid pH 3 and incubation for 1 minute at RT followed by the addition of PBS (pH 7.4) to neutralized acidic pH. Next, reaction mixture was applied to a 1 mL HiTrap KappaSelect affinity column (GE Healthcare Life Sciences). All affinity purification steps were carried out by connecting the affinity column to a peristaltic pump with flow rate of 1ml/min. The reaction mixture was recycled three times through the KappaSelect column to maximize the capture of intact mAb and mAb-F(ab')$_2$. KappaSelect column was subsequently washed with 5CV of PBS and eluted with 10CV of 100mM glycine·HCl (pH 2.7). Collected 1ml elution fractions were immediately neutralized with 100µl of 1.5M Tris·HCl (pH 8.8). Next, the recovered intact mAb and mAb-F(ab')$_2$ fragments were applied to a custom packed 1ml Protein-G agarose column (GenScript). The reaction mixture was recycled three times through the column, which was subsequently washed with 5CV of PBS and eluted with 10CV of 100mM glycine·HCl (pH 2.7). The 10ml elution fraction was immediately neutralized with 1ml of 1.5M Tris·HCl (pH 8.8). The recovered 10ml mAb-F(ab')$_2$ fragments were dialyzed overnight at 4°C against 4L of PBS (pH 7.4) using SnakeSkin dialysis tubing with 10kDa cutoff (Thermo Fisher Scientific). Recovered mAb-F(ab')$_2$ sample were evaluated for purity by SDS-PAGE and their concentration measured by Take5 (BioTek instruments).

To test the functionality of the produced mAb-F(ab')$_2$, 96 ELISA plates (Nunc MaxiSorp™ flat-bottom, Thermo Fisher Scientific) were coated with 1µg/ml of rhTNFα in PBS and incubated at 4°C O.N. ELISA plates were then washed three times with PBST and blocked with 300µl of 2% w/v BSA in PBS for 1 hour at 37^{o}C. Next, 50nM of intact mAb and mAb-F(ab')$_2$ (IFX or ADL) in blocking solution was added to each well in triplicates in a 3 fold dilution series, and plates were incubated at RT for 1 hour. Next, plates were washed three times with PBST with 30 second incubation time at each washing cycle. For detection, HRP conjugated anti-human kappa light chain (Jackson) was added to each well (50µl, 1:5000 ratio in 2% w/v BSA in PBS) and incubated

for 1 hour at RT, followed by three washing cycles with PBST. Developing was carried out by adding 50µl of TMB and reaction was quenched by adding 0.1M sulfuric acid. Plates were read using the Epoch Microplate Spectrophotometer ELISA plate reader. To evaluate the purity of the mAb-Fa(b')$_2$ samples (i.e. to make sure there are no traces of intact antibody or Fc fragment in the sample) , 96 ELISA plate (Nunc MaxiSorp™ flat-bottom, Thermo Fisher Scientific) were coated with 5µg/ml of intact mAb and mAb-F(ab')$_2$ in PBS and incubated at 4°C O.N. Next, plates were washed three time with PBST and blocked with 300µl 2% w/v BSA in PBS for 1 hour at 37°C. Next, plates were washed three times with 300 µl PBST, followed by the incubation with HRP conjugated anti-human IgG Fc antibody (Jackson) diluted 1:5000 in PBST. Developing was carried out by adding 50µl of TMB and reaction was quenched by adding 0.1M sulfuric acid. Plates were read using the Epoch Microplate Spectrophotometer ELISA plate reader (BioTek Instruments).

Generation of ADA standard

A pool of 17 ADA to IFX positive sera were collected at Sheba Medical Center, and passed through a 2ml custom packed protein G agarose column (GenScript). The pooled sera was recycled three times over the column, which was subsequently washed with 5CV of PBS and eluted with 10CV of 100mM glycine·HCl (pH 2.7). The 10ml elution fraction was immediately neutralized with 1ml of 1.5M Tris·HCl (pH 8.8). The purified mAbs were immediately passed over a custom made rhTNFα affinity column (NHS-activated agarose beads, Thermo Fisher Scientific) in gravity mode. The purified mAbs were recycled three times over the column, which was subsequently washed with 5CV of PBS and eluted with 10CV of 100mM glycine·HCl (pH 2.7). The 10ml elution fraction was immediately neutralized with 1ml of 1.5M Tris·HCl (pH 8.8). The purified mAbs were dialyzed overnight at 4°C against 4L of PBS (pH 7.4) using SnakeSkin dialysis tubing with 10kDa cutoff (Thermo Fisher Scientific). Purified mAbs were analyzed for purity using 12% SDS-PAGE and concentration was determined by Take3 (BioTek instruments).

To test functionality, 96 ELISA plate were coated with 5µg/ml of mAb-F(ab')$_2$ in PBS (pH 7.4) and incubated at 4°C O.N. ELISA plates were then washed three times with PBST and blocked with 300µl of 2% w/v BSA in PBS for 1 hour at 37°C. Next, 50nM of the purified ADA in blocking solution were added to each well in triplicates with 3-fold dilution series and plates were incubated at RT for 1 hour. Next, plates were washed three times with PBST with 30 second incubation time at each washing cycle. Next, anti-human Fc HRP conjugate (Jackson) was added to each well at the detection phase (50µl, 1:5000 ratio in 2% w/v BSA in PBS) and incubated for

1 hour at RT, followed by three washing cycles with PBST. Developing was carried out by adding 50µl of TMB and reaction was quenched by adding 0.1M sulfuric acid. Plates were read using the Epoch Microplate Spectrophotometer ELISA plate reader.

Quantitative measurement of ADA in serum

The schematic configuration of the bio-immunoassay for the quantitative measurement of ADA in serum is described in Fig. 3B and was carried out as follows: ELISA plates that were coated overnight at 4°C with 5µg/ml produced IFX-F(ab')$_2$ in PBS (pH 7.4). ELISA plates were then washed three times with PBST and blocked with 300µl of 2% w/v BSA in PBS for 1 hour at 37^{o}C. Next, triplicates of 1:400 diluted serum samples were added at triplicates and serially diluted 2 fold in 2% w/v BSA in PBS, 10% horse serum (Biological Industries) and 1% Tween 20 in PBS (1:400– 1:51,200 serum dilution factor). Plates were incubated for 1 hour at RT. On the same plate, serial dilutions of 10nM ADA standard were incubated in triplicate and serially diluted 2 fold in 2% w/v BSA in PBS, 10% horse serum (Biological Industries) and 1% Tween 20 in PBS, to allow the conversion of the tested serum to units per milliliter. ELISA plates were washed three times with PBST and 50µl of HRP conjugated anti-human IgG Fc was added to each well (50µl, 1:5000 ratio in 2% w/v BSA in PBS) and incubated for 1 hour at RT. ELISA plate was then washed three times with PBST and developed by adding 50µl of TMB followed by quenching with 50µl 0.1M sulfuric acid. Plates were read using the Epoch Microplate Spectrophotometer ELISA plate reader.

Neutralization index of ADA

Neutralization capacity was determined using ELISA plates that were coated overnight at 4°C with 5µg/ml IFX-F(ab')$_2$ in PBS (pH 7.4 ELISA plates were then washed three times with PBST and blocked with 300µl of 2% w/v BSA in PBS for 1 hr at 37^{o}C. Next, triplicates of 1:400 diluted serum samples were added to the negative TNFα wells and serially diluted 2 fold in 2% w/v BSA in PBS, 10% horse serum (Biological Industries) and 1% Tween 20 in PBS. Triplicates of 1:400 diluted serum samples with 200nM rhTNFα were also added to the remaining wells and serially diluted 2 fold in 2% w/v BSA in PBS, 10% horse serum (Biological Industries) and 1% Tween 20 in PBS (1:400– 1:51,200 serum dilution factor). Plates were incubated for 1 hour at RT. ELISA plates were washed three times with PBST and 50µl of HRP conjugated anti-human IgG Fc

antibody or anti HRP conjugated His-tag antibody were added at the detection phase (50µl, 1:5000 ratio in 2% w/v BSA in PBS) and incubated for 1 hour at RT, followed by three washing cycles with PBST. Developing was carried out by adding 50µl of TMB and reaction was quenched by adding 0.1M sulfuric acid. Plates were read using the Epoch Microplate Spectrophotometer ELISA plate reader. Neutralization index was calculated by the logarithmic score of triplicate average differences between the ELISA equation curve without rhTNFα and in the presence of rhTNFα where the value of the control background is above 3-x standard deviation.

Blood processing

IFX treated patients with IBD cared for in the Department of Gastroenterology at the Sheba medical center were included in the study. All subjects signed an informed consent, and the study was approved by the Ethics Committee of the medical center. All patients received IFX on a scheduled regimen and blood samples were drawn immediately before their scheduled IFX infusion. Blood was collected into a single Vacutainer Lithium Heparin collection tube (BD Bioscience).

For NGS analysis, blood was collected from a male donor treated with IFX, before IFX administration and 10 days after administration. 30ml of peripheral blood were collected into 3 single Vacutainer K-EDTA collection tubes (BD Biosciences). Collection of peripheral blood mono-nuclear cells (PBMCs) was performed by density gradient centrifugation, using Uni-SepMAXI+ lymphocyte separation tubes (Novamed) according to the manufacturer's protocol.

Fluorescence-Activated Cell Sorting Analysis and sorting of B cell populations

PBMCs were stained for 15 minutes in cell staining buffer (BioLegend) at RT in the dark using the following antibodies: anti-CD3–PerCP (clone OKT3; BioLegend), anti-CD19– Brilliant Violet 510 (clone HIB19; BioLegend), anti-CD27–APC (clone O323; BioLegend), anti-CD38–APC-Cy7 (clone HB-7; BioLegend), and anti-CD20–FITC (clone 2H7; BioLegend).

The following B cell population was sorted using a FACSAria cell sorter (BD Bioscience): CD3−CD19+CD20-CD27++CD38^{high}

B cell subpopulations were sorted and collected into TRI Reagent solution (Sigma Aldrich) and frozen at −80°C.

Amplification of V_H and V_L repertoires from B cells

Total RNA was isolated using RNeasy micro Kit (Qiagen), according to manufacturer's protocol. First-strand cDNA generation was performed with 100ng of isolated total RNA using a SuperScript RT II kit (Invitrogen) and oligo-dT primer, according to manufacturer's protocol. After cDNA synthesis, PCR amplification was performed to amplify the V_H and V_L genes using a primer set described previously (25) with overhang nucleotides to facilitate Illumina adaptor addition during the second PCR (Table S1). PCR reactions were carried out using FastStart™ High Fidelity PCR System (Roche) with the following cycling conditions: 95°C denaturation for 3 min; 95°C for 30 sec, 50°C for 30 sec, and 68°C for 1 min for four cycles; 95°C for 30 sec, 55°C for 30 sec, and 68°C for 1 min for four cycles; 95°C for 30 sec, 63°C for 30 sec, and 68°C for 1 min for 20 cycles; and a final extension at 68°C for 7 min. PCR products were purified using AMPure XP beads (Beckman Coulter), according to manufacturer's protocol (ratio x 1.8 in favor of the beads). Recovered DNA products from the first PCR was applied to a second PCR amplification to attach Illumina adaptors to the amplified V_H and V_L genes using the primer extension method as described previously (31). PCR reactions were carried out using FastStart™ High Fidelity PCR System (Roche) with the following cycling conditions: 95°C denaturation for 3 min; 95°C for 30 sec, 40°C for 30 sec, and 68°C for 1 min for two cycles; 95°C for 30 sec, 65°C for 30 sec, and 68°C for 1 min for 7 cycles; and a final extension at 68°C for 7 min. PCR products were applied to 1% agarose DNA gel electrophoresis and gel-purified with Zymoclean™ Gel DNA Recovery Kit (Zymo Research) according to the manufacturer's instructions. V_H and V_L libraries concentration were measured using Qubit system (Thermo Fisher Scientific) and library quality was assessed using the Bioanalyzer 2100 system (Agilent) or the 4200 TapeStation system (Agilent). All V_H libraries were produced in duplicates starting with RNA as the common source template. The V_L were produced with one replicate.

V_H and V_L libraries from sorted B cell were subjected to NGS on the MiSeq platform with the reagent kit V3 2x300 bp paired-end (Illumina), using an input concentration of 16pM with 5% PhiX.

Raw fastq files were processed using our recently reported ASAP webserver (29). ASAP analysis resulted in a unique, full-length V_H and V_L gene sequences database for each time point. The resultant database was used as a reference database to search the LC-MS/MS spectra.

Proteomic Analysis of the Serum ADA to IFX

Total IgG from each time point (D0, D10) were purified from 7-10ml of serum by protein G enrichment. Serum was diluted 2 fold and passed through a 5ml Protein G agarose column (GeneScript). The diluted serum was recycled three times over the column, which was subsequently washed with 10CV of PBS and eluted with 7CV of 100mM glycine·HCl (pH 2.7). A total of 35 fractions of 1ml were collected and immediately neutralized with 100µl of 1.5M Tris·HCl (pH 8.8). All elution fractions were evaluated for their purity using 12% SDS–PAGE and 11 purified 1 ml IgG fractions were combined and dialyzed overnight at 4°C against 4L of PBS (pH 7.4) using SnakeSkin dialysis tubing with 1 kDa cutoff (Thermo Fisher Scientific).

Next, 9mg of total IgG were digested with 100µg of IdeS in the final volume of 2ml PBS for 5 hour at 37^0C. IdeS inactivation was carried out by adding 0.1M of citric acid pH 3 and incubation for 1 minute at RT followed by the addition of PBS (pH 7.4) to neutralize the low pH. Total serum $F(ab')_2$ was then applied to a one ml custom made affinity column comprised of IFX-$F(ab')_2$ coupled to NHS-activated agarose beads (Thermo Fisher Scientific). The purified serum $F(ab')_2$ were recycled three times over the affinity column, which was subsequently washed with 5CV of PBS and eluted with 15CV of 100mM glycine·HCl (pH 2.7) and collected into Maxymum Recovery Eppendorf (Axygen Scientific). A total of 30x0.5ml elution fractions and 1x50ml flow-through were immediately neutralized with 50 and 100µl (respectively) of 1.5M Tris·HCl (pH 8.8). The purified antigen-specific $F(ab')_2$ were dialyzed overnight at 4°C against 4L of PBS (pH 7.4) using SnakeSkin dialysis tubing with 10kDa cutoff (Thermo Fisher Scientific). Elution and flow-through fractions were trypsin-digested, and resulting peptides were fractionated and sequenced by nanoflow LC-electrospray MS/MS on an Orbitrap Velos Pro hybrid mass spectrometer (Thermo Scientific), in the UT Austin mass spectrometry core facility as described previously (38). MS/MS raw files were analyzed by MaxQuant software version 1.6.0.16 (46) using the MaxLFQ algorithm (47) and peptide lists were searched against the common contaminants database by the Andromeda search engine (48) and a custom protein sequence database consisting of the donor-specific V_H and V_L sequences derived from NGS of individual donor B cells. All searches were carried out with cysteine carbamidomethylation as a fixed modification and methionine oxidations as variable modifications. The false discovery rate was set to 0.01 for peptides with a minimum length of seven amino acids and was determined by searching a reverse decoy database. Enzyme specificity was set as C-terminal to arginine and lysine as expected using trypsin as protease, and a maximum of two missed cleavages were allowed in the database search. Peptide identification was performed with an allowed initial precursor mass deviation up to 7ppm and an allowed fragment mass deviation of 20ppm. For LFQ

quantification the minimal ratio count was set to 2, and match between runs was performed with three mass-spec injections originating from the same sample. MaxQunat output analysis file, "peptides.txt", was used for further processing. Total peptides that were identified in the elution samples were filtered using the following criteria: (a) were not identified as contaminates; (b) did not match to the reversed decoy database; (c) were identified as peptides derived from the region comprising the CDRH3, J region, FR4 and the ASTK motif (derived from the N-terminal of the C_H1 region). The CDRH3 derived peptides were further characterized as informative CDRH3 peptides (*i*CDRH3 peptides) only if they map exclusively to a single antibody clonotype. A clonotype was defined as all sequences that comprise CDRH3 with the same length and identity tolerating one amino acid mismatch, and same V, J family. The intensities of high confidence *i*CDRH3 peptides were averaged between replicates while including only peptides that were observed in at least two out of the three replicates. Clonotype frequencies within each sample were calculated using only *i*CDRH3 peptides and were determined to be antigen-specific if their frequency in the elution fraction was at least 5 fold greater than their frequency in the flow-through fraction. The CDRH3 sequences identified by the mapping of high confidence MS/MS peptides were used to generate a complete list of full length VH sequences. These VH sequences were used to analyze the repertoire measures of the antibodies that were identified in the donors' serum.

Study population

IFX and ADL treated patients with IBD cared for in the Departments of Gastroenterology at Sheba medical center were included in the study. All subjects signed an informed consent, and the study was approved by the Ethics Committee of Sheba medical center. IFX and ADL and ADA serum levels were routinely measured at trough immediately before infusion. All patients received IFX and ADL on a scheduled regimen. All patients that were included in this study exhibited low through levels of IFX and ADL.

Statistical analysis

All curves were fitted on a sigmoidal dose–response curve and EC50 of each was calculated. Mann-Whitney test was used to compare continuous variables. All reported P values were two-tailed, and a P value less than 0.05 were considered statistically significant. All statistics were performed with GraphPad Prism software (version 7, San Diego, California).

Results

Production of mAb-F(ab')$_2$ to be used in the bio-immunoassay

To investigate the molecular landscape of ADA following mAb administration we first aimed to develop an accurate, sensitive, robust bio-immunoassay to determine ADA levels in sera. The working hypothesis was that anti-idiotypic antibodies dominate the ADA compartment (21) thus, the developed bio-immunoassay was based on the drugs' F(ab')$_2$ portion to be used as the antigen (i.e. coating agent).

To achieve this, we used the immunoglobulin G (IgG)-cleaving enzyme (IdeS), a cysteine proteinase enzyme that proteolytically cleaves immunoglobulins below the hinge region (22) (Figure 1A). IFX was digested using IdeS by incubating 10 mg of clinical grade mAb with IdeS to reach near complete digestion. Next, IFX-F(ab')$_2$ was purified from Fc regions and undigested full IFX by consecutive affinity chromatography steps comprising protein A and kappaSelect columns.

Recovered IFX-F(ab')$_2$ purity was evaluated by SDS-PAGE (Figure 1B) and ELISA (Figure 1C) to ensure that the IFX-F(ab')$_2$ exhibits no traces of IFX-Fc/undigested IFX that will contribute to the background level when using anti-Fc HRP conjugate at the detection phase. Recovered IFX-F(ab')$_2$ samples were found to be highly pure with basal anti-Fc signal levels similar to the signal observed in the control samples. The produced IFX-F(ab')$_2$ was tested for functionality by measuring its TNFα binding capacity, using ELISA with TNFα as the coating agent, and was found to show similar functionality as that of the intact IFX (Figure 1D). ADL was subjected to the same preparative pipeline and demonstrated similar results (Figure S1).

ADA Standard curve

Quantification of total ADA in serum requires a standard reference. Thus, we generated a standard ADA pool that facilitates the quantification of ADA levels in sera of patient treated with IFX. ADA were pooled from several serum samples collected from patients treated with IFX and purified by consecutive affinity chromatography steps comprising protein G and a custom-made IFX-F(ab')$_2$ affinity columns. We confirmed the affinity enrichment of ADA by applying the affinity chromatography elution fraction to ELISA with IFX-F(ab')$_2$ as the coated antigen (Figure 2A). The purity and concentration the recovered ADA were determined by SDS-PAGE (Figure 2B) and nanodrop.

Maximal serum concentration used in a bio-immunoassay (e.g. serum diluted 1:100 or 1:200) is a major factor that may contribute to high background signal levels due to non-specific binding. Screening several maximal serum dilutions showed that 1:400 initial serum dilution demonstrates the lowest background signal (data not shown). To evaluate if serum will affect the signal obtained from purified ADA, we spiked-in purified ADA into negative control serum that was diluted 1:400 in PBS. Serial dilution of spiked-in ADA and purified ADA showed similar signal in ELISA (Figure 2C) indicating that serum does not bias the ADA detection in our developed bio-immunoassay.

Quantitative measurement of ADA in serum

ADA detection is technically challenging as both the analyte and antigen are antibodies which may result in the inability to differentiate between the mAb and ADA. To overcome this challenge, many assays were previously developed (5). One of these immunoassays is the anti-human λ chain (AHLC) immunoassay that is used in clinical setups for monitoring the formation of ADA (23). The principle of this assay is to detect ADA comprising λ light chain, thus avoiding cross reactivity with the drug that comprises the κ light chain (Figure 3A).

While AHLC is suitable for monitoring the development of ADA in clinical setups, when one aims to study the molecular composition of ADA there is a need to provide quantitative measures of total ADA in serum. Thus, we developed a new bio-immunoassay based on the $F(ab')_2$ portion of the mAb. The bio-immunoassay setup is described in Figure 3B and is based on mAb-$F(ab')_2$ as the coating antigen and anti-Fc HRP conjugate used as the detection antibody. Each of the experimental setups to test ADA in serum included serum from a healthy donor as a control and ADA standard for the quantitation of total ADA.

First, we applied the newly developed bio-immunoassay on two serum sample groups: one negative and one positive for ADA as determined by the AHLC assay ($AHLC^{(-)}$ and $AHLC^{(+)}$, respectively). We also included serum from a healthy subject to serve as a control for the assay specificity (i.e. serum from a subject that was not exposed to IFX). As shown in Figure 3C-D, the ELISA signals obtained when utilizing the new bio-immunoassay were higher compared to the signal obtained with the AHLC assay. Moreover, applying the new bio-immunoassay on the $AHLC^{(-)}$ serum (no detected ADA with the AHLC assay) detected relatively high levels of ADA. These results indicate that not all ADA were detected with the AHLC assay as this assay is based on the detection of ADA that comprise the λ light chain only.

Next, to extend and generalize the above results, sera from 55 patients treated with IFX were collected at the Chaim Sheba Medical Center and tested for drug levels and ADA using the AHLC assay. The established cohort showed very low drug trough levels and based on the AHLC results, sera were stratified into two groups: 26 serum samples were identified as $AHLC^{(-)}$ and 29 as $AHLC^{(+)}$. Using our newly developed quantitative bio-immunoassay, we found that ADA levels in tested sera ranged between 2.7 to 1268.5 µg/ml. Serum ADA levels using AHLC compared to the new bio-immunoassay are summarized in Table 1. More importantly, the new bio-immunoassay demonstrated improved sensitivity compared to AHLC assay manifested in the detection of higher concentrations of ADA in 40 out of the 55 serum samples, of which 12 out of the 55 samples, belong to the $AHLC^{(-)}$ group. Overall, the average fold increase in ADA detection using the new bio-immunoassay compared to the AHLC assay was 17.3 and 60.6 for the $AHLC^{(+)}$ and $AHLC^{(-)}$ groups , respectively.

Neutralization index of ADA

Due to high clinical relevance and different mechanism of action of *b*ADA and *nt*ADA, identifying their relative abundances in serum can provide valuable insights regarding the nature of the immune response following mAb administration. We therefore modified our newly developed mAb-$F(ab')_2$ based bio-immunoassay by blocking the coated IFX-$F(ab')_2$ binding site with TNFα in order to obtain a differential signal compared to the unblocked assay (Figure 4A). In order to block the binding site of IFX-$F(ab')_2$ towards TNFα and prevent the binding of anti-idiotypic ADA (i.e. *nt*ADA) to the drug, recombinant human TNFα (rhTNFα) fused to a His-tag was cloned and expressed (see materials and methods). In-house production of rhTNFα was essential, as the N terminal His-tag was used for monitoring the presence of the rhTNFα throughout the bio-immunoassay.

First, we evaluated the ability of rhTNFα to inhibit the binding of ADA to the coated IFX-$F(ab')_2$ by setting up a competitive ELISA where a series of ADA standard concentrations were incubated with a series of fixed rhTNFα concentrations (data no shown). We observed a competitive effect while rhTNFα was fixed at the concentration of 5nM (Figure 4B). This step was important as it enabled us to determine the ADA equimolar concentration of rhTNFα to be used that will fully occupy the IFX-$F(ab')_2$ binding site and will prevent the binding of *nt*ADA to the coated (and blocked) IFX-$F(ab')_2$. We monitored the presence of rhTNFα using an HRP-conjugated anti-His tag antibody and observed that if we aim to completely block ADA it is

505 required to use equimolar concentration of rhTNFα that is corresponds to the highest
506 concentration of ADA in the assay (200nm).

507 In practice, IFX-F(ab')$_2$ binding site was blocked with rhTNFα by prior incubation of serum with
508 the coated IFX-F(ab')$_2$ hence, the differential signal w/ and w/o the presence of rhTNFα represent
509 the portion of ADA that could not bind the IFX-F(ab')$_2$ binding site thus, reflects the
510 neutralization capacity (hereby named neutralization index) of the ADA in the tested serum.
511 Using this assay, we evaluated the neutralization index of the 55 sera from patients treated with
512 IFX and 7 sera from patients treated with ADL. In sera from patients treated with IFX, we noticed
513 that there are two main neutralization index patterns: those with high differential signal (Figure
514 5A) and low differential signal (Figure 5B). More interestingly, we found that patients that were
515 stratified as AHLC$^{(+)}$ have a significantly higher neutralization index compared to those that
516 belong to the AHLC$^{(-)}$ group (Figure 5C). This suggests that there is a preferential usage of the
517 λ light chain in *nt*ADA as the AHLC$^{(+)}$ group is *a priori* defined by the presence of ADA
518 comprising the λ light chains. All sera from patients treated with ADL (n=7) were subjected to
519 modified bio-immunoassay and demonstrated high neutralization indexes (Figure S2)

520

521 **IFX infusion induces a vaccine like immune response**

522 To further investigate the molecular landscape of ADA we explored the dynamics of the B cell
523 response following mAb administration. When investigating well-controlled clinical scenarios
524 such as samples obtained from post-vaccinated individuals, it is convenient to isolate the antigen-
525 specific B cell as they peak at a defined time window (24, 25). However, the characteristics of the
526 humoral response and ADA encoding B cell dynamics following mAb administration is unknown.
527 Our working hypothesis assumed that the immune response following mAb administration is a
528 vaccine-like response thus; we expected to observe a wave of PB peaking several days after IFX
529 infusion. It was previously demonstrated that boost vaccines induce a strong proliferation of PBs
530 and mBCs that can be detected in the blood circulation several days after the boost (26, 27). To
531 test if IFX administration induces a vaccine like response, we collected blood samples from a
532 patient that was found to be positive to ADA at two time points: prior to IFX infusion (D0) and 10
533 days after IFX infusion (D10). The second time point (D10) was determined in order to capture an
534 enriched population of antigen-specific PB as well as mBC that enable the establishment of a
535 donor-specific V_H database for the proteomic interpretation of peptides derived from ADA.

Peripheral blood mononuclear cells (PBMCs) were sorted by FACS and the frequency of PB ($CD3^-CD19^+CD20^-CD27^{++}CD38^{++}$) and mBC ($CD3^-CD19^+CD20^+CD27^+$) subsets were determined. We identified a 13-fold increase in the frequency of PB at D10 and no increase in the mBC compartment. The PB data suggests that the B cell dynamics following IFX infusion exhibits vaccine-like characteristics in accordance with our working hypothesis (Table 2, Figure S3).

Antibody repertoire of ADA encoding B-Cells

The waves of PB following challenge is enriched with antigen-specific B cells (24, 25, 28). Based on this, a major fraction of PB at D10 post mAb infusion is expected to comprise B cell clones responding to the current antigen challenge. Thus, the repertoire of B cells at two time points (pre- and post-infusion) is predicted to represent the overall differences in the ongoing ADA encoding B cell response.

This diversity of antibodies is accomplished by several unique molecular mechanisms, including chromosomal V(D)J rearrangement, somatic hypermutations (SHM) and class switch recombination (29), processes that are mediated by recombination-activating gene (RAG) and activation-induced cytidine deaminase (AID), respectively. The AID enzyme functions mainly in secondary lymph nodes named germinal centers. Next-generation sequencing (NGS) of the antibody variable regions (V-genes) coupled with advanced bioinformatics tools provides the means to elucidate the antigen-specific antibody repertoire's immense diversity (30). To deep sequences antibodies' V-genes, recovered RNA from sorted PB and mBC was used as the template for first-strand cDNA synthesis, followed by PCR amplification steps to produce barcoded amplicons of the V-genes of the antibody heavy chains (V_H) as described previously (31). While NGS of antibodies is a powerful tool for immune repertoire analysis, relatively high rates of errors accumulate during the experimental procedure. To overcome this challenge, we generated duplicates of the antibody V-gene amplicons and sequenced them using the Ilumina MiSeq platform (2x300bp). The resultant V_H sequences were processed using our recently reported ASAP webserver that was specifically developed to analyze NGS of antibody V-gene sequences derived from replicates (29).

In our analysis, we concentrated on several repertoire measures that collectively provide a molecular level characterization of the ADA: i) V(D)J family usage; ii) CDR3 length distribution; iii) SHM levels, and, iv) isotype distribution. Our data revealed several interesting antibody

repertoire features that may shed light on the molecular mechanism involved in the formation of ADA.

V(D)J gene family usage is stable

Examining the V(D)J family usage is important to determine whether the basal gene frequency is similar to the expected frequency and if the B cell response following IFX infusion drives B cells to exhibit a preferential V(D)J gene usage. Therefore, we examined the frequency of family usage at two time points (D0 and D10), within PB and mBC subsets across isotypes (IgG and IgM). The V(D)J family usage showed no marked difference between the two time points, B cell subsets and isotypes. The frequency of V-gene family usage was also found to have similar frequency profile as previously described (32, 33). For example, the V-gene family frequency showed that the V3, V4 and V1 have the most prevalent representation followed by V2, V5 and V6 that had significantly lower frequencies (Figure 6A). The same pattern trends were identified for the D and J family usage.

CDRH3 length increases following IFX infusion

Composed of the V(D)J join with its inherent junctional diversity, the CDRH3 specifies the antibody V_H clonotype. The V_H clonotype is an important immunological concept because it accounts for antibodies that likely originate from a single B-cell lineage and may provide insight on the evolution of the antigen-specific response (34). Here we defined V_H clonotype as the group of V_H sequences that share germ-line V and J segments and have identical CDRH3 sequences. By examining the length distribution of CDRH3 from PB across isotypes and time point we observed a shift towards longer CDRH3 at D10 (Figure 7). Interestingly, this observation is in contrast to previous studies that reported a decrease in the CDRH3 length post immunization with pneumococcal (35) and hepatitis B vaccines (36) and when comparing antigen experienced B cell to naïve B cells (37).

Somatic hypermutation levels decreases following IFX infusion

Examining the level of SHM following vaccination provides insights regarding the extent of the affinity maturation that antigen-stimulated B cell undergo. It was previously reported that boost vaccination induces a substantial increase of the SHM levels when comparing post- to pre-vaccination (36). Despite the vaccine like response following IFX infusion, we observed in the

PB compartment a significant decrease in the SHM levels post-infusion, regardless if the mutations were synonymous and non-synonymous (Figure 8).

Proteomic analysis of ADA

Analysis of serum antibodies provides a comprehensive profile of the humoral immune response and is complementary to the transcriptomic analysis derived from NGS of the antibody V_H. Applying an approach that integrates NGS and tandem mass spectrometry (LC-MS/MS) has been shown to provide valuable data regarding the composition of antigen-specific serum antibodies and their relationship to B cells and generates new insights regarding the development of the humoral immune response in disease and following vaccination (24, 25). Here we utilized the previously developed omics approach (34, 38) to elucidate the serum ADA composition following IFX infusion. ADA from 10 ml of serum collected at D0 and D10 were subjected to protein G affinity chromatography and total of 9 mg of recovered IgG was digested by IdeS to remove the Fc regions that may mask the MS/MS signal obtained from low abundant peptides. Following 5 hours of digestion, the reaction mixture was subjected to custom made affinity column where the IFX-F(ab')$_2$ was coupled to agarose beads and served as the antigen to isolate ADA. Recovered 48.57µg polyclonal ADA-F(ab')$_2$ (i.e., IFX-F(ab')$_2$-specific IgG's) in the elution fraction and total F(ab')$_2$ (depleted from ADA-F(ab')$_2$) in the flow through fraction were digested with trypsin and injected to high-resolution tandem mass spectrometer analyzer in triplicates. LC-MS/MS raw data files were analyzed using MaxQuant using label free quantitation mode (LFQ) and searched against the custom antibody V-gene database derived from the NGS data of B cells isolated from the same donor. Identified peptide from the interpretation of the proteomic spectra were stratified into three types of peptides: informative peptides (*i*Peptide) that map uniquely to one antibody clonotype in a region that is upstream to the CDRH3, non-informative CDRH3 peptides (*ni*CDRH3) that map to the CDRH3 region of the antibody but do not map uniquely to a single antibody clonotype and informative CDRH3 peptides (*i*CDRH3) that map uniquely to a single antibody clonotype. Summary of identified peptides in LC-MS/MS are shown in Table 3. Beyond the designation as *i*CDRH3 peptides, additional filtration steps were applied including peptides that were present in more than 2 replicates, peptides in elution that show 5xfold frequency than in the flow through. The *i*CDRH3 peptides enabled the identification of 62 unique ADA CDRH3 clonotypes with 205 associated full-length V-gene sequences. The resulting V-gene sequences were analyzed to determine their V(D)J family usage and the B cell subset they are mapped to, based on our NGS data (Figure 9).

The V(D)J family usage of the antibody variable region sequences that were identified by LC-MS/MS (Figure 9A) showed a similar distribution as observed in the NGS data (Fig. 6A, Fig. 7A). V family frequency analysis showed that the V1, V3, and V4 are the most dominant V families followed by V2 and V5 that had significantly lower frequencies. D family frequency analysis showed that the D6, D3, D2 and D1 have the most prevalent representation, and J family frequency showed that the J4, J5 and J6 have the most prevalent representation.

Next, we examined the distribution of the proteomically identified V-gene sequences to B cell subsets (Figure 9B) and found that the V-genes predominantly map to mBC from D0 (46.83%), followed by mBC from D10 (27.8%). Moreover, we found that 23.9% of V-genes map to D10 PB. Based on the dynamics of antibodies in serum (24), the majority of antibodies produced following a boost challenge are the product of pre-existing mBC cells that were re-activated following drug infusion, much like a response to a vaccine boost (25).

As mentioned above, flow cytometry of B cells following IFX administration allowed us to identify a substantial increase in the frequency of PB at D10, which suggests that the B cell dynamics following IFX infusion exhibits vaccine-like characteristics. Therefore, we expected to find a majority of V-gene sequences mapping to IgG^+ B cells that underwent class switch recombination in the germinal center. Surprisingly, the majority of proteomically identified serum antibodies were mapped to IgM^+ B cells (Figure 9C).

Next, we aimed to provide support to the observation that *nt*ADA preferably use the λ light chain. By quantifying the accumulative intensities of peptides derived from the constant region of both light chains we calculate the change in the ratio between peptide that were derived from the affinity chromatography elution fraction (ADA) and the flow through fraction (non-ADA). The expected κ/λ ratio of total IgG in serum is 2 (66% κ and 33% λ). Indeed, proteomic analysis of the affinity chromatography flow through fractions (D0 and D10) that represent the total IgG population depleted from ADA, resulted in average κ/λ ratio of 2.1. The same analysis of the elution fraction showed a significant shift of the κ/λ ratio to 1.19. These data support our serological data that ntADA preferably use the λ light chain and thus, contribute to the shift in the κ/λ ratio.

Discussion

The use of therapeutic mAbs in treating a wide range of diseases and disorders is growing exponentially. Nonetheless, a major shortcoming of their use is the development of ADA in patients receiving the mAb. Advances in mAb engineering have enabled the development of fully human mAbs with reduced immunogenicity without abolishing it completely. Thus a mAb administered to a patient can still induce an immune sensitization as reflected by the production of ADA, which is associated with low trough drug levels and can mediate loss of clinical response to the drug (20).

The precise mechanism underlying ADA production is unknown, and many questions related to its development remain unaddressed, including determining precise concentrations of ADA in serum, which portion of the ADA exhibits neutralizing capacity, the immune pathway governing the production of ADA, and ultimately, the molecular composition of ADA at the sequence level. To address these questions, we chose the chimeric TNFα antagonist IFX as the model system. First, we aimed to quantify the ADA level in patient sera. Many methods were previously reported to evaluate serum ADA levels; however, those assays provide mostly qualitative measures to assist physicians in deciding the most appropriate intervention when treating patients, and many (if not all) studies underestimated actual ADA levels (19). To provide quantitative measures describing the molecular landscape of ADA, we first developed a bio-immunoassay that would allow quantify ADA levels based on the $F(ab')_2$ region of the mAb because previous reports indicated that the ADA generated from mAb administration are mostly anti-idiotypic (21). Indeed, the bio-immunoassay demonstrated higher sensitivity compared with the AHLC assay used initially to detect ADA and was able to detect ADA when the AHLC assay could not. Leveraging its improved sensitivity, we applied our proprietary assay on sera from 55 patients treated with IFX and found that patients designated as $AHLC^{(+)}$ showed significantly higher levels of ADA (mean: 264 μg/ml) compared to the $AHLC^{(-)}$ group (mean: 57 μg/ml). These results support the clinical use of AHLC assay because overall, patients were correctly stratified leading to clinical decision-making that was based on a valid indicative assay. Notwithstanding, the applicability of the AHLC assay, the newly developed $F(ab')_2$-based bio-immunoassay demonstrated that ADA levels can reach extreme concentrations that were not detected using the AHLC assay.

Some patients who develop ADA in response to IFX present a prolonged remission with maintenance therapy despite repeated indications of high ADA and low IFX trough levels (20). The mechanism of action of these ADA has significant influence on drug efficacy. For example,

*b*ADA are most likely to enhance the clearance of a drug whereas *nt*ADA will prevent a drug from binding to its target. Hence, it is important to differentiate between *b*ADA and *nt*ADA, or in other words, a need exists to identify sera with high levels of *nt*ADA that may predict the likelihood of a patient losing a favorable response to an administrated mAb. To achieve this, we further revised our bio-immunoassay to qualitatively measure the neutralization index of ADA in the serum of patients treated with IFX. Using this assay on sera from the 55 patients, revealed that patients who tested positive utilizing the AHLC assay, exhibit a significantly higher neutralization index than patients tested negatively for it (i.e., $AHLC^{(-)}$). Noteworthy, the AHLC assay is based on the anti-λ light chain antibody at the detection stage, suggesting that ADA with high neutralization index preferably use the λ light chain. This phenomenon received additional support from our proteomic analysis in which we compared the changes in the ratio between peptides derived from κ and λ constant light chains from IFX-specific IgG pool and peptide derived from total IgG polyclonal pool. This analysis demonstrated that the κ/λ ratio in the total IgG compartment is as expected and is decreased in the mAb-specific compartment (κ/λ ratio 2.1 and 1.19 for total IgG and ADA, respectively). The preferential use of the λ light chain in neutralizing antibodies has been previously reported (21, 39), however, the authors of those studies did not provide an explanation beyond the structural adaptability of the light chain toward the target. The relevance of the reported cases showing λ chain bias is not clear. Similar phenomena was reported in B-1 sub-population, unlike follicular B cells, B-1 cells exhibit an increased frequency of lambda light chains (40). The recurrence of BCRs with the enrichment of λ light chain has been considered to result from strong antigen-dependent selection of the B-1 cell repertoire (41).

Repetitive administration of mAbs may induce a strong humoral response manifested in the production of ADA. We hypothesized that mAb administration is similar to the response that occurs following a boost vaccine. Others and we have demonstrated that boost vaccines induce a strong proliferation of PB that can be detected in blood circulation several days after the boost. The “wave” of B cells after the boost vaccine are dominated by antigen-specific B cell (27) thus, repertoire analysis of these cells can provide invaluable data about the antigen-specific antibody repertoires. Utilizing flow cytometry showed an order of magnitude increase in PB compartment 10 days after IFX infusion, suggesting that the immune response following IFX administration is indeed similar to a vaccine response. To the best of our knowledge, this is the first report to identify a vaccine like response following therapeutic mAb administration.

Next, we aimed to provide a comprehensive repertoire profile of the B cells induced after mAb administration. To achieve this, we applied an "omics" approach as previously described (25, 34, 38) that is based on the integration of NGS of the V-genes and proteomic analysis of serum ADA. NGS of V-genes revealed no bias in the V(D)J usage across isotypes, cell types, and time point. These data suggest that the original repertoire that existed before mAb administration and antigen-specific repertoire induced by IFX administration is formed by random recombination processes without preferential use of any particular V(D)J segment. Comparative repertoire analysis of the V-genes between time points (before and after IFX administration) revealed that post-IFX administration, PB exhibit longer CDRH3 and lower SHM rates. Although the B cell dynamics after mAb administration are similar to those that occur after a boost vaccine, the repertoire measures show a different profile. It was previously reported that the antibodies generated after a boost vaccine exhibit shorter CDRH3, high SHM (35-37).

To explain these data we revisited two reports: the first describes how the immune response in TNFα-deficient mice was "diverted" to the marginal zone instead of to the germinal center (42) and the characteristics of the immune response in the marginal zone is directly affected by low levels of the AID that in turn is reflected in lower SHM rate. The second reported a skewed λ chain usage in B-1 cells (40). Based on these reports we propose a mechanistic model according to which administration of TNFα antagonist blocks the TNFα on one hand and induces a vaccine-like response on the other. Due to the TNFα blockade, immune response of B cells occurs extra follicular where AID is downregulated, thus the encoded ADA exhibit lower SHM rates. Moreover, the data suggests that the immune response following mAb administration may be a T cell independent (TI) response which is governed by the B1 cell linage with the characteristics mentioned of an increased usage of λ light chains and little to non-evidence for SHM (40, 43).

Another possible mechanism that should be further explored is the strong TI immune response in the marginal zone that is also induced by a drug/ADA immune-complex (IC). It was previously suggested that many of the immune-mediated adverse effects attributed to ADA require the formation of an IC intermediate that can have a variety of downstream effects (6, 44).In the context of the system we investigated, administration of a TNFα antagonist will divert the immune response extra follicular either by TNFα blockade or by the formation of an IC carrying multiple mAbs that can induce the cross-linking of cognate BCR. The BCR of ADA-encoding B cells will undergo co-clustering leading to their activation in the TI pathway.

In our study we examined molecular aspects related to the formation of ADA. To the best of our knowledge, this is the first report describing ADA repertoire that resulted in insights about a possible mechanism of ADA formation. Further work will be needed to elucidate additional phenotypic markers of the B cells induced by mAb administration and the role of IC in the activation of the B cell. Moreover, the mechanism described here covers the response to a TNFα-antagonist, and by using the same omics approaches it will be highly informative to study the B cell response following treatment with other mAbs.

762 **Acknowledgments**

763 **General**: We are grateful to George Georgiou for assisting with the LC-MS/MS measurements at UT Austin, for
764 Ulrich von Pawel-Rammingen from the Department of Molecular Biology, Umea University who kindly donated the
765 plasmid with the gene encoding the IdeS.

766 **Funding:** The work was partially supported by BSF grant 2017359 (Y.W.)

767 **Author contributions:** A.V.M, S.B.H, I.B. and Y.W. conceived the research. A.V.M. S.R. and Y.W. designed the
768 experiments, A.V.M., S.R., M.Y., E.F. and Y.D. performed experiments, A.V.M., S.R., S.B.H, M.Y., E.F., B.U. and
769 U.K. collected and processed clinical samples, A.V.M, A.K. and Y.W. carried out data analysis, A.V.M. and Y.W.
770 wrote the manuscript.

771 **Competing interests:** The authors declare no competing financial interests.

772 **This manuscript has been released as a Pre-Print at BioRxiv. DOI:**

773

774 **References**
775
776
777 **References**
778
779 1. Grilo AL, Mantalaris A. The Increasingly Human and Profitable Monoclonal Antibody
780 Market. *Trends in biotechnology* (2019) 37(1):9-16. doi: 10.1016/j.tibtech.2018.05.014.
781 2. van Schouwenburg PA, Rispens T, Wolbink GJ. Immunogenicity of anti-TNF biologic
782 therapies for rheumatoid arthritis. *Nat Rev Rheumatol* (2013) 9(3):164-72. doi:
783 10.1038/nrrheum.2013.4.
784 3. De Groot AS, Scott DW. Immunogenicity of protein therapeutics. *Trends in immunology*
785 (2007) 28(11):482-90. doi: 10.1016/j.it.2007.07.011.
786 4. Hansel TT, Kropshofer H, Singer T, Mitchell JA, George AJ. The safety and side effects
787 of monoclonal antibodies. *Nat Rev Drug Discov* (2010) 9(4):325-38. doi: 10.1038/nrd3003.
788 5. Bloem K, Hernandez-Breijo B, Martinez-Feito A, Rispens T. Immunogenicity of
789 Therapeutic Antibodies: Monitoring Antidrug Antibodies in a Clinical Context. *Ther Drug Monit*
790 (2017) 39(4):327-32. doi: 10.1097/FTD.0000000000000404.
791 6. Krishna M, Nadler SG. Immunogenicity to Biotherapeutics - The Role of Anti-drug
792 Immune Complexes. *Frontiers in Immunology* (2016) 7. doi: 10.3389/fimmu.2016.00021.
793 7. Nelson AL, Dhimolea E, Reichert JM. Development trends for human monoclonal
794 antibody therapeutics. *Nat Rev Drug Discov* (2010) 9(10):767-74. doi: 10.1038/nrd3229.
795 8. Ben-Horin S, Heap GA, Ahmad T, Kim H, Kwon T, Chowers Y. The immunogenicity of
796 biosimilar infliximab: can we extrapolate the data across indications? *Expert Rev Gastroenterol*
797 *Hepatol* (2015) 9 Suppl 1:27-34. doi: 10.1586/17474124.2015.1091307.
798 9. Bendtzen K. Immunogenicity of Anti-TNF-α Biotherapies: II. Clinical Relevance of
799 Methods Used for Anti-Drug Antibody Detection. *Frontiers in Immunology* (2015) 6:109. doi:
300 10.3389/fimmu.2015.00109.
301 10. Putnam WS, Prabhu S, Zheng Y, Subramanyam M, Wang Y-MC. Pharmacokinetic,
302 pharmacodynamic and immunogenicity comparability assessment strategies for monoclonal
303 antibodies. *Trends in biotechnology* (2010) 28(10):509-16. doi: 10.1016/j.tibtech.2010.07.001.
304 11. Sands BE, Anderson FH, Bernstein CN, Chey WY, Feagan BG, Fedorak RN, et al.
305 IInfliximab maintenance therapy for fistulizing Crohn's disease. *New England Journal of*
306 *Medicine* (2004) 350(9):876-85. doi: 10.1056/NEJMoa030815.
307 12. Mitoma H, Horiuchi T, Hatta N, Tsukamoto H, Harashima S, Kikuchi Y, et al. Infliximab
308 induces potent anti-inflammatory responses by outside-to-inside signals through transmembrane
309 TNF-alpha. *Gastroenterology* (2005) 128(2):376-92.
310 13. Ben-Horin S, Vande Casteele N, Schreiber S, Lakatos PL. Biosimilars in Inflammatory
311 Bowel Disease: Facts and Fears of Extrapolation. *Clin Gastroenterol Hepatol* (2016)
312 14(12):1685-96. doi: 10.1016/j.cgh.2016.05.023.
313 14. Baker MP, Reynolds HM, Lumicisi B, Bryson CJ. Immunogenicity of protein
314 therapeutics: The key causes, consequences and challenges. *Self Nonself* (2010) 1(4):314-22. doi:
315 10.4161/self.1.4.13904.
316 15. Ungar B, Engel T, Yablecovitch D, Lahat A, Lang A, Avidan B, et al. Prospective
317 Observational Evaluation of Time-Dependency of Adalimumab Immunogenicity and Drug
318 Concentrations: The Poetic Study. *The American journal of gastroenterology* (2018) 113(6):890-
319 8. doi: 10.1038/s41395-018-0073-0.
320 16. Ungar B, Chowers Y, Yavzori M, Picard O, Fudim E, Har-Noy O, et al. The temporal
321 evolution of antidrug antibodies in patients with inflammatory bowel disease treated with
322 infliximab. *Gut* (2014) 63(8):1258-64. doi: 10.1136/gutjnl-2013-305259.

17. Vincent FB, Morand EF, Murphy K, Mackay F, Mariette X, Marcelli C. Antidrug antibodies (ADAb) to tumour necrosis factor (TNF)-specific neutralising agents in chronic inflammatory diseases: a real issue, a clinical perspective. *Ann Rheum Dis* (2013) 72(2):165-78. doi: 10.1136/annrheumdis-2012-202545.
18. Tatarewicz S, Miller JM, Swanson SJ, Moxness MS. Rheumatoid factor interference in immunogenicity assays for human monoclonal antibody therapeutics. *J Immunol Methods* (2010) 357(1-2):10-6. doi: 10.1016/j.jim.2010.03.012.
19. Bloem K, van Leeuwen A, Verbeek G, Nurmohamed MT, Wolbink GJ, van der Kleij D, et al. Systematic comparison of drug-tolerant assays for anti-drug antibodies in a cohort of adalimumab-treated rheumatoid arthritis patients. *J Immunol Methods* (2015) 418:29-38. doi: 10.1016/j.jim.2015.01.007.
20. Ben-Horin S, Chowers Y. Tailoring anti-TNF therapy in IBD: drug levels and disease activity. *Nature reviews Gastroenterology & hepatology* (2014) 11(4):243-55. doi: 10.1038/nrgastro.2013.253.
21. Ben-Horin S, Yavzori M, Katz L, Kopylov U, Picard O, Fudim E, et al. The immunogenic part of infliximab is the F(ab′)2, but measuring antibodies to the intact infliximab molecule is more clinically useful. *Gut* (2010) 60(1):gut.2009.201533-48. doi: 10.1136/gut.2009.201533.
22. von Pawel-Rammingen U, Johansson BP, Björck L. IdeS, a novel streptococcal cysteine proteinase with unique specificity for immunoglobulin G. *The EMBO Journal* (2002) 21(7):1607-15. doi: 10.1093/emboj/21.7.1607.
23. Kopylov U, Mazor Y, Yavzori M, Fudim E, Katz L, Coscas D, et al. Clinical utility of antihuman lambda chain-based enzyme-linked immunosorbent assay (ELISA) versus double antigen ELISA for the detection of anti-infliximab antibodies. *Inflammatory bowel diseases* (2012) 18(9):1628-33. doi: 10.1002/ibd.21919.
24. Lee J, Boutz DR, Chromikova V, Joyce MG, Vollmers C, Leung K, et al. Molecular-level analysis of the serum antibody repertoire in young adults before and after seasonal influenza vaccination. *Nature Medicine* (2016) 22(12):1456-+. doi: 10.1038/nm.4224.
25. Lavinder JJ, Wine Y, Giesecke C, Ippolito GC, Horton AP, Lungu OI, et al. Identification and characterization of the constituent human serum antibodies elicited by vaccination. *Proceedings of the National Academy of Sciences of the United States of America* (2014) 111(6):2259-64. doi: 10.1073/pnas.1317793111.
26. Haney DJ, Lock MD, Gurwith M, Simon JK, Ishioka G, Cohen MB, et al. Lipopolysaccharide-specific memory B cell responses to an attenuated live cholera vaccine are associated with protection against Vibrio cholerae infection. *Vaccine* (2018) 36(20):2768-73.
27. Davydov AN, Obraztsova AS, Lebedin MY, Turchaninova MA, Staroverov DB, Merzlyak EM, et al. Comparative Analysis of B-Cell Receptor Repertoires Induced by Live Yellow Fever Vaccine in Young and Middle-Age Donors. *Front Immunol* (2018) 9:2309. doi: 10.3389/fimmu.2018.02309.
28. Blanchard-Rohner G, Pulickal AS, der Zijde CMJ-v, Snape MD, Pollard AJ. Appearance of peripheral blood plasma cells and memory B cells in a primary and secondary immune response in humans. *Blood* (2009) 114(24):4998-5002. doi: 10.1182/blood-2009-03-211052.
29. Avram O, Vaisman-Mentesh A, Yehezkel D, Ashkenazy H, Pupko T, Wine Y. ASAP, A Webserver for Immunoglobulin-Sequencing Analysis Pipeline. *Frontiers in Immunology* (2018) 9. doi: 10.3389/fimmu.2018.01686.
30. Greiff V, Menzel U, Haessler U, Cook SC, Friedensohn S, Khan TA, et al. Quantitative assessment of the robustness of next-generation sequencing of antibody variable gene repertoires from immunized mice. *BMC immunology* (2014) 15(1):40. doi: 10.1186/s12865-014-0040-5.
31. Menzel U, Greiff V, Khan TA, Haessler U, Hellmann I, Friedensohn S, et al. Comprehensive Evaluation and Optimization of Amplicon Library Preparation Methods for High-Throughput Antibody Sequencing. *PLOS ONE* (2014) 9(5). doi: 10.1371/journal.pone.0096727.

32. Mroczek ES, Ippolito GC, Rogosch T, Hoi KH, Hwangpo TA, Brand MG, et al. Differences in the composition of the human antibody repertoire by B cell subsets in the blood. *Frontiers in immunology* (2014) 5:96-. doi: 10.3389/fimmu.2014.00096.
33. Volpe JM, Kepler TB. Large-scale analysis of human heavy chain V(D)J recombination patterns. *Immunome research* (2008) 4:3-. doi: 10.1186/1745-7580-4-3.
34. Wine Y, Boutz DR, Lavinder JJ, Miklos AE, Hughes RA, Hoi KH, et al. Molecular deconvolution of the monoclonal antibodies that comprise the polyclonal serum response. *Proc Natl Acad Sci USA* (2013) 110(8):2993-8. doi: 10.1073/pnas.1213737110.
35. Ademokun A, Wu YC, Martin V, Mitra R, Sack U, Baxendale H, et al. Vaccination-induced changes in human B-cell repertoire and pneumococcal IgM and IgA antibody at different ages. *Aging cell* (2011) 10(6):922-30. doi: 10.1111/j.1474-9726.2011.00732.x.
36. Galson JD, Trück J, Fowler A, Clutterbuck EA, Münz M, Cerundolo V, et al. Analysis of B Cell Repertoire Dynamics Following Hepatitis B Vaccination in Humans, and Enrichment of Vaccine-specific Antibody Sequences. *EBioMedicine* (2015) 2(12):2070-9. doi: https://doi.org/10.1016/j.ebiom.2015.11.034.
37. DeKosky BJ, Lungu OI, Park D, Johnson EL, Charab W, Chrysostomou C, et al. Large-scale sequence and structural comparisons of human naive and antigen-experienced antibody repertoires. *Proc Natl Acad Sci U S A* (2016) 113(19):E2636-45. doi: 10.1073/pnas.1525510113.
38. Boutz DR, Horton AP, Wine Y, Lavinder JJ, Georgiou G, Marcotte EM. Proteomic Identification of Monoclonal Antibodies from Serum. *Analytical Chemistry* (2014) 86(10):4758-66. doi: 10.1021/ac4037679.
39. Robinson JE, Hastie KM, Cross RW, Yenni RE, Elliott DH, Rouelle JA, et al. Most neutralizing human monoclonal antibodies target novel epitopes requiring both Lassa virus glycoprotein subunits. *Nature communications* (2016) 7:11544-. doi: 10.1038/ncomms11544.
40. Hayakawa K, Hardy RR, Herzenberg LA. Peritoneal Ly-1 B cells: genetic control, autoantibody production, increased lambda light chain expression. *Eur J Immunol* (1986) 16(4):450-6. doi: 10.1002/eji.1830160423.
41. Rowley B, Tang L, Shinton S, Hayakawa K, Hardy RR. Autoreactive B-1 B cells: constraints on natural autoantibody B cell antigen receptors. *J Autoimmun* (2007) 29(4):236-45.
42. Pasparakis M, Alexopoulou L, Episkopou V, Kollias G. Immune and inflammatory responses in TNF alpha-deficient mice: a critical requirement for TNF alpha in the formation of primary B cell follicles, follicular dendritic cell networks and germinal centers, and in the maturation of the humoral immune response. *Journal of Experimental Medicine* (1996) 184(4):1397-411. doi: 10.1084/jem.184.4.1397.
43. Kantor AB, Herzenberg LA. Origin of murine B cell lineages. *Annu Rev Immunol* (1993) 11:501-38. doi: 10.1146/annurev.iy.11.040193.002441.
44. Bar-Yoseph H, Pressman S, Blatt A, Vainberg SG, Maimon N, Starosvetsky E, et al. Infliximab-Tumor Necrosis Factor Complexes Elicit Formation of Anti-drug Antibodies. *Gastroenterology* (2019) In Press. doi: 10.1053/j.gastro.2019.08.009.
45. Wenig K, Chatwell L, von Pawel-Rammingen U, Björck L, Huber R, Sondermann P. Structure of the streptococcal endopeptidase IdeS, a cysteine proteinase with strict specificity for IgG. *Proceedings of the National Academy of Sciences of the United States of America* (2004) 101(50):17371-6. doi: 10.1073/pnas.0407965101.
46. Cox J, Mann M. MaxQuant enables high peptide identification rates, individualized p.p.b.-range mass accuracies and proteome-wide protein quantification. *Nature biotechnology* (2008) 26(12):1367-72. doi: 10.1038/nbt.1511.
47. Cox J, Hein MY, Luber CA, Paron I, Nagaraj N, Mann M. Accurate proteome-wide label-free quantification by delayed normalization and maximal peptide ratio extraction, termed MaxLFQ. *Molecular & cellular proteomics : MCP* (2014) 13(9):2513-26. doi: 10.1074/mcp.M113.031591.

48. Cox J, Neuhauser N, Michalski A, Scheltema RA, Olsen JV, Mann M. Andromeda: a peptide search engine integrated into the MaxQuant environment. *Journal of proteome research* (2011) 10(4):1794-805. doi: 10.1021/pr101065j.

Figure legends

Figure 1: IFX digestion and IFX-F(ab')$_2$ purification. (A) Schematic representation of IgG digestion with IdeS. IdeS is a highly specific immunoglobulin-degrading enzyme that cleaves below the disulfide bonds in the IgG hinge region. The cleavage results in the production of IFX-F(ab')$_2$ fragment and two ½ Fc fragments. (B) SDS-PAGE analysis of intact IgG (lane 2), following IdeS digestion (lane 3) and purified IFX-F(ab')$_2$ following a 2-step affinity chromatography purification including protein A and kappa-select columns (lane 4). (C) Presence of Fc and intact IgG traces was measured by direct ELISA where intact IFX and purified IFX-F(ab')$_2$ were compared to a control antigen (streptavidin) as coating agents followed by direct incubation with an anti-Fc HRP conjugate at the detection phase. (D) The functionality of the recovered IFX-F(ab')$_2$ was confirmed by testing it for TNFα binding by ELISA in comparison to intact IFX. The ELISA setup included TNFα as the coating agent and anti- HRP conjugate at the detection phase. For panel C–D, triplicate averages were calculated as mean, with error bars indicating s.d.

Figure 2: Standard curve for ADA quantification in patients treated with IFX. ADA were purified from sera of 17 patients treated with IFX, utilizing consecutive affinity chromatography steps including protein G and custom made IFX-F(ab')$_2$ columns. (A) Purified ADA were tested in ELISA for functionality. TNFα was used as the coating agent followed by incubation with purified ADA and anti-Fc HRP conjugate at the detection phase. Control included serum obtained from a healthy donor. (B) SDS-PAGE analysis of intact IFX (lane 2) and purified ADA (lane 3). (C) The effect of serum on ADA standard was tested in ELISA by s piking-in differential concentrations of ADA into ADA negative serum.

Figure 3: AHLC and the newly developed mAb-F(ab')$_2$ based bio-immunoassay configuration and their application on serum samples from patients treated with IFX. (A) AHLC assay is based on an ELISA where TNFα is used as the coating agent, following the incubation with the mAb drug followed by serial dilutions of the tested sera. anti-λ HRP conjugate is used at the detection phase. (B) The newly developed mAb-F(ab')$_2$ based bio-immunoassay configuration. The assay is based on an ELISA where mAb-F(ab')$_2$ is used as the coating agent followed by serial dilutions of the tested sera. Anti-Fc HRP conjugate is used at the detection phase. (C) ELISA obtained by utilizing the AHLC assay on two serum samples. Using this assay, one of the tested sera showed detectable levels of ADA (AHLC$^{(+)}$) and one had no detectable levels of ADA (AHLC$^{(-)}$). (D) Both serum samples were tested by the newly developed mAb-F(ab')$_2$ based bio-immunoassay. This assay was able to detect ADA in both sera. For C–D, averages were calculated as mean from triplicates, with error bars indicating s.d.

Figure 4: Configuration of the assay for determining the neutralization index of ADA in patient sera and competitive ELISA between ADA and rhTNFα. (A) The newly developed mAb-F(ab')$_2$ based bio-immunoassay configuration (left) and the modified configuration where mAb-F(ab')$_2$ binding site is blocked by saturating the assay with rhTNFα (right). (B) Competitive effect of rhTNFα on ADA binding to IFX-F(ab')$_2$. ELISA plate was coated with 5μg/ml of IFX-F(ab')$_2$. ADA standard was diluted 3-fold in blocking solution supplemented with 5nM rhTNFα. ADA diluted 3-fold in blocking solution without the presence of rhTNFα served as a control.

Figure 5: Neutralization index ELISA. (A) Graph representing the ELISA results obtained utilizing the neutralization assay on serum sample that show detectable levels of ADA (AHLC$^{(+)}$) and (B) serum sample with no detectable levels of ADA (AHLC$^{(-)}$). (C) Scatter plot consolidating the neutralization index obtained by applying the immunoassay on sera from 55 patients treated with IFX (***P = 0.0003, Mann-Whitney U test). For B–C, averages were calculated as mean, with error bars indicating s.d.

Figure 6: V, D and J family usage in B cell following IFX infusion. mBC and PB from a patient treated with IFX were collected at two time points (D0, D10) and processed for NGS analysis. The V family usage showed no difference between D0 and D10, different B cell subsets and isotypes. The D and J family usage showed no difference between time points.

Figure 7: **CDRH3 length at two time point and across isotypes**. PB from a patient treated with IFX were collected at two time points (D0, D10) and processed for NGS analysis. An increase in antibody CDRH3 length was observed. (***P<0.001, Mann-Whitney U test).

Figure 8: Somatic hyper mutations. PB from a patient treated with IFX were collected at two time points (D0, D10) and processed for NGS analysis. A decrease in the number of Ka mutations (number of non-synonymous mutation per codon) and Ks mutations (number of synonymous mutations per codon) was observed at D10. (****P<0.0001, Mann-Whitney U test).

Figure 9: V-gene and circulating antibody repertoire characteristics. (A) The V(D)J family usage of V-gene sequences that were identified by LC-MS/MS. (B) Mapping of V-gene sequences to B cell subsets and (C) isotypes, based on NGS data.

Table 1: ADA concentrations in 55 serum samples from patients treated with IFX. Serum samples were initially stratified into AHLC (+) and AHLC (-) based on the AHLC assay used in the clinic. The newly developed bio-immunoassay for the quantification of total ADA was applied on all serum samples and concentration are listed. All ADA concentrations are in µg/ml.

AHLC$^{(-)}$ patients			AHLC$^{(+)}$ patients		
Patient #	AHLC	New bio-immunoassay µg/ml	Patient #	AHLC	New bio-immunoassay µg/ml
5645	0	867.33	14655	7.9	121.95
5557	0.9	0	15046	16.6	85.24
5381	1.9	0	15460	21.1	147.89
6497	1.6	26.26	15809	22.8	996.84
6386	1.7	0	15107	6.3	126.5
6259	0.8	41.39	14408	4.8	90.54
6098	1.3	0	4297	8.9	274.6
5993	1.3	0	5048	5.6	49.28
5912	1.8	0	5735	6.9	99.67
5882	1.7	152.72	6393	3.4	289.31
5822	1.3	0	6324	6.7	91.14
6291	0.7	19.43	6275	31.8	242.03
6616	0.3	84.05	6261	27.2	245.52
7083	1	97.29	6208	5.8	65.35
7041	1	0	6165	3	2.7
7004	0.7	4.28	6148	7.2	148.88
6866	1.3	80.05	9348	42.2	285.05
6788	1.8	46.83	8970	59.3	1268.5
6740	1.5	0	8816	27.2	396.2
14735	0.4	0	7553	46.7	178.83
14752	1.2	43.87	12113	20.9	772.83
14879	1.7	0	12104	20.9	441.09
14834	0.57	0	6329	11	87.31
13741	1.3	18	8178	7.9	55.11
13711	0.3	0	7653	16.1	53.52
14278	1.72	0	8856	42.4	87.97
			9454	7.8	265.35
			12343	16.5	358.54
			12345	37	329.49

Table 2: B cell frequency of a patient treated with IFX.

Time point	B cell subset	% Frequency of sorted cells (out of CD19+ cells)	No. of raw paired-end sequencing reads		No. of filtered paired-end sequencing reads			No. of unique IGH clonotypes extracted (Unique CDRH3)
			Replicate A	Replicate B	Replicate A	Replicate B	Joint	
D0	PB	0.9%	39,129	63,168	12,863	19,082	2041	1294
	mBC	10%	714,722	639,984	121,998	111,373	30,725	9146
D10	PB	11.5%	167,859	151,849	49,762	46,192	10,341	5590
	mBC	9.7%	528,765	488,619	143,864	133,879	40,899	19,521

Table 3: Summary of identified peptides and the corresponding clonotype and antibody somatic variences in the LC-MS/MS spectra. E: elution, FT: flow-through.

	Day 0	Day 10
Total peptides	908	3177
Total antibody peptides	761	2805
Total CDRH3	42	224
Present in ≥2 technical replicates	30	166
Frequency ratio E/FT > 5	11	81
№ of clones	5	62
№ of somatic variances	35	205

Figure 1

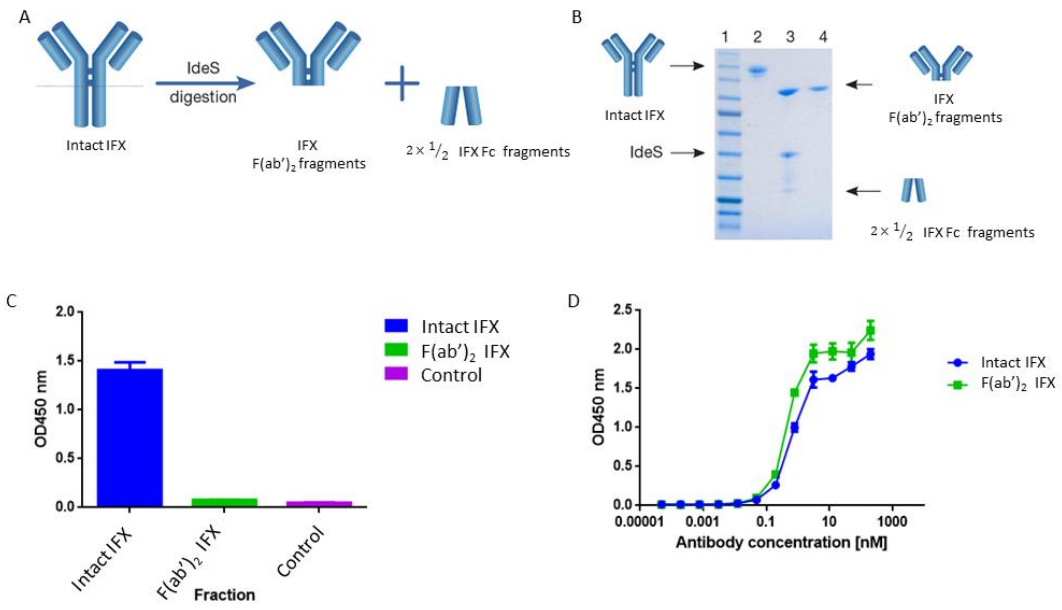

Figure 2

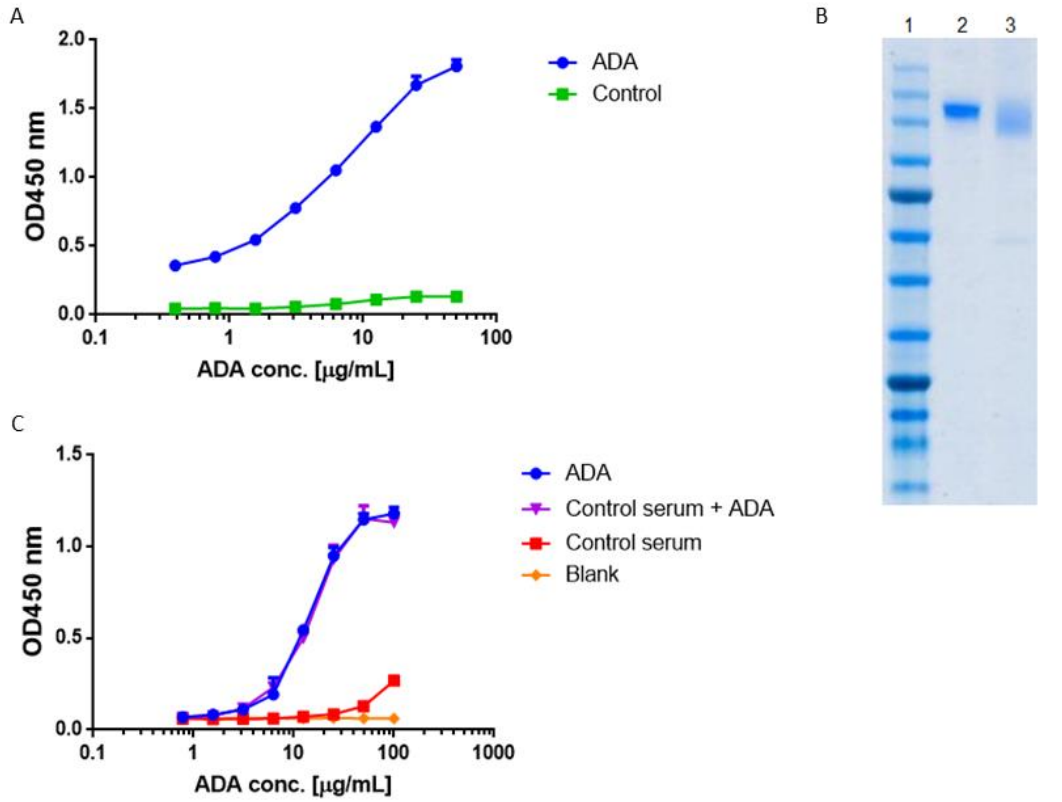

Figure 3

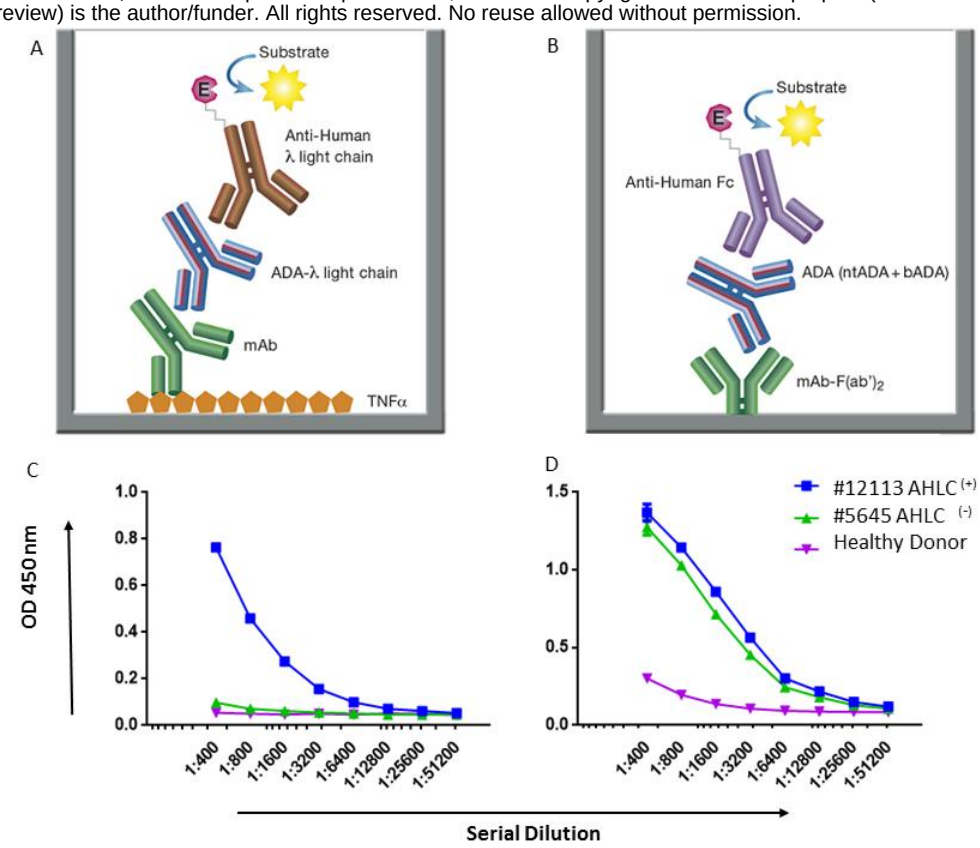

Figure 4

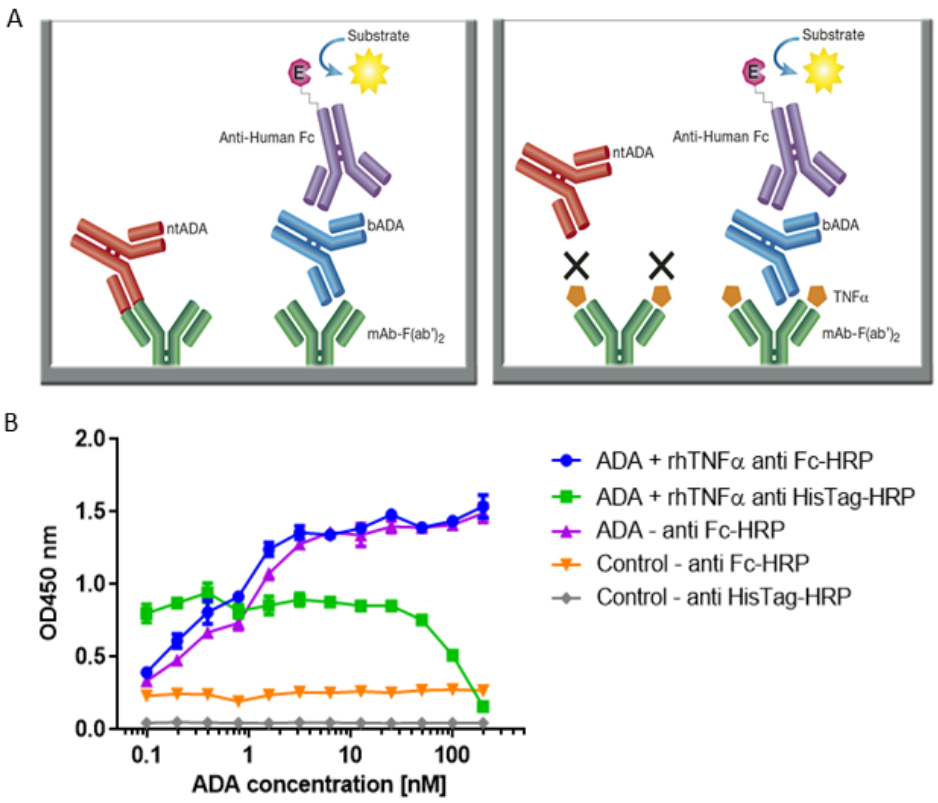

Figure 5

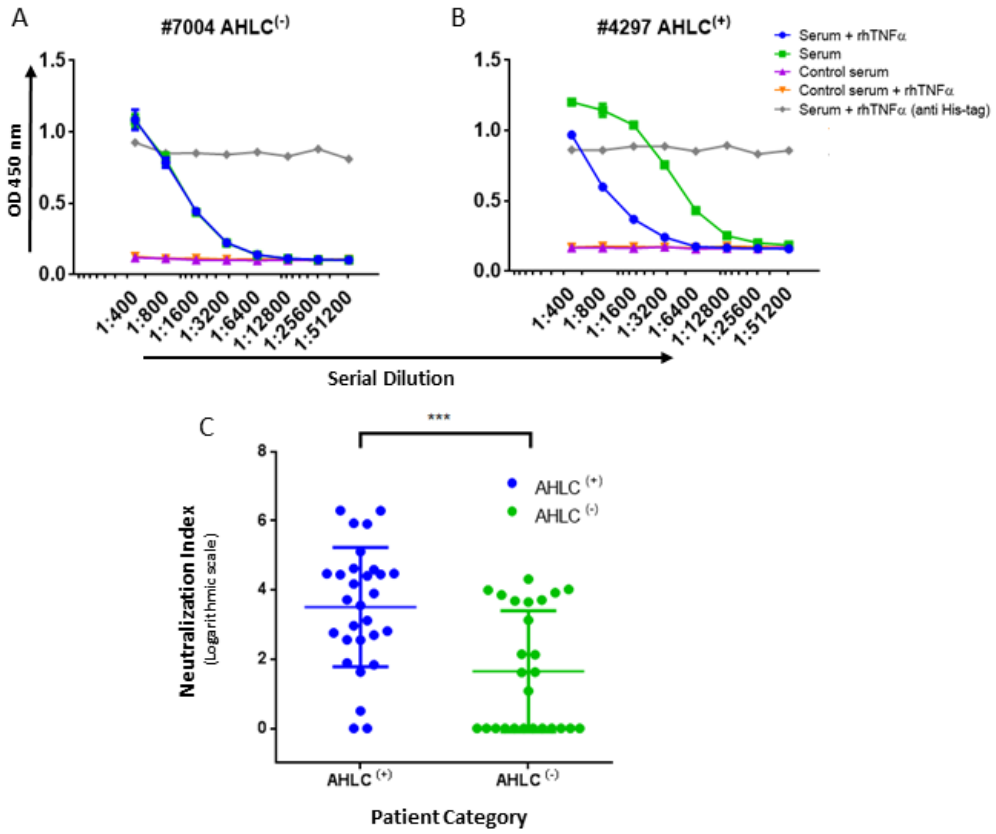

Figure 6

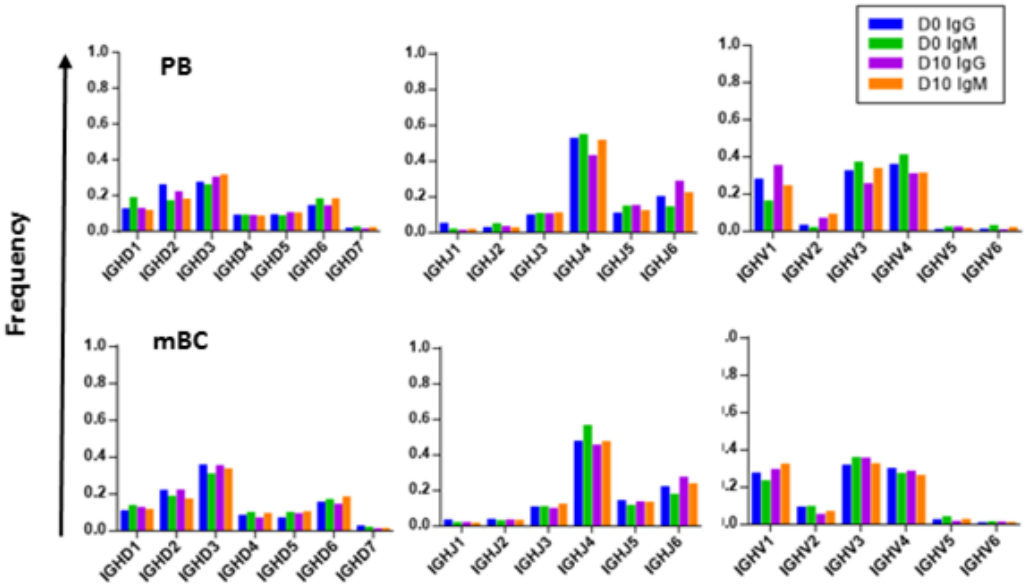

Figure 7

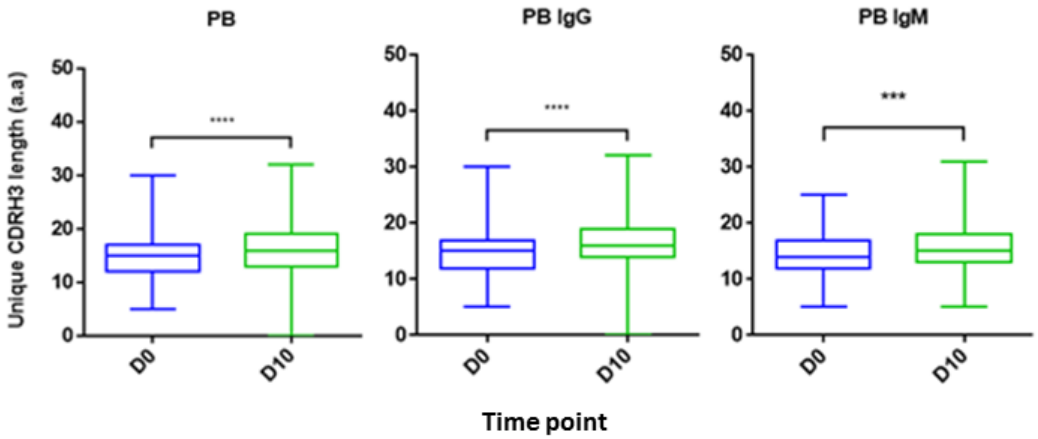

Figure 8

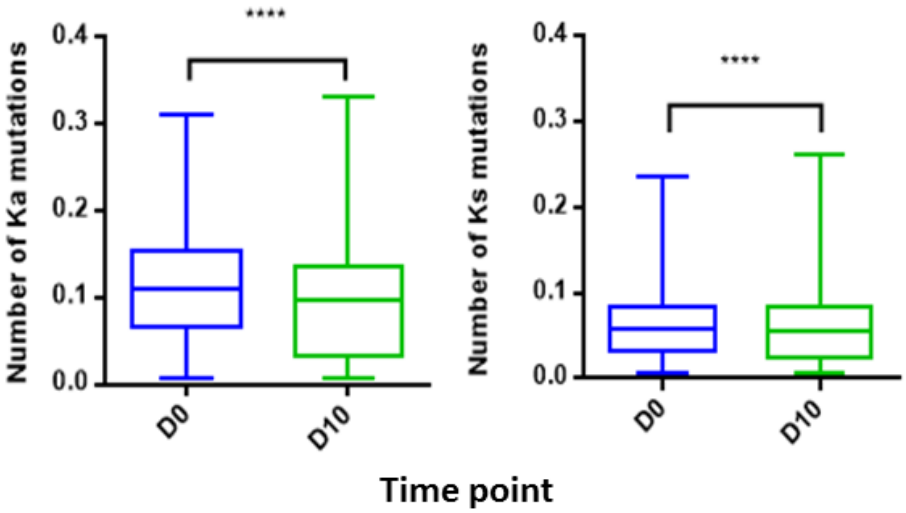

Figure 9